Spring 2011

ESTIMATION OF LAND SURFACE EVAPOTRANSPIRATION WITH A SATELLITE REMOTE SENSING PROCEDURE

Ayse Kilic
University of Nebraska-Lincoln, akilic@unl.edu

Ian Ratcliffe
University of Nebraska-Lincoln, iratcliffe2@unl.edu

Pariskhit Ranade
University of Nebraska-Lincoln, ranade.p.k@gmail.com

Kenneth Hubbard
University of Nebraska-Lincoln, khubbard1@unl.edu

Ramesh K. Singh
USGS Earth Resources Observation and Science (EROS) Center, Sioux Falls, SD
See next page for additional authors

Authors
Ayse Kilic, Ian Ratcliffe, Pariskhit Ranade, Kenneth Hubbard, Ramesh K. Singh, Babuarao Kamble, and Jeppe Kjaersgaard

Great Plains Research 21 (Spring 2011):73–88

ESTIMATION OF LAND SURFACE EVAPOTRANSPIRATION WITH A SATELLITE REMOTE SENSING PROCEDURE

Ayse Irmak

School of Natural Resources and the Department of Civil Engineering
311 Hardin Hall
University of Nebraska–Lincoln
Lincoln, NE 68583-0973
airmak2@unl.edu

Ian Ratcliffe and **Pariskhit Ranade**

School of Natural Resources
231 Hardin Hall
University of Nebraska–Lincoln
Lincoln, NE 68583-0973

Kenneth G. Hubbard

School of Natural Resources
703 Hardin Hall
University of Nebraska–Lincoln
Lincoln, NE 68583-0997

Ramesh K. Singh

USGS Earth Resources Observation and Science (EROS) Center
47914 252nd Street
Sioux Falls, SD 57198

Babuarao Kamble

Department of Civil Engineering
231 Hardin Hall
University of Nebraska–Lincoln
Lincoln, NE 68583-0973

and

Jeppe Kjaersgaard

Kimberly R&E Center
University of Idaho
3793 North 3600 East
Kimberly, ID 83341-5076

ABSTRACT—There are various methods available for estimating magnitude and trends of evapotranspiration. Bowen ratio energy balance system and eddy correlation techniques offer powerful alternatives for measuring land surface evapotranspiration. In spite of the elegance, high accuracy, and theoretical attractions of these techniques for measuring evapotranspiration, their practical use over large areas can be limited due to the number of sites needed and the related expense. Application of evapotranspiration mapping from satellite measurements can overcome the limitations. The objective of this study was to utilize the METRIC™ (Mapping

Manuscript received for review, April 2009; accepted for publication, September 2010.

Evapotranspiration at High Resolution using Internalized Calibration) model in Great Plains environmental settings to understand water use in managed ecosystems on a regional scale. We investigated spatiotemporal distribution of a fraction of reference evapotranspiration (ETrF) using eight Landsat 5 images during the 2005 and 2006 growing season for path 29, row 32. The ETrF maps generated by METRIC™ allowed us to follow the magnitude and trend in ETrF for major land-use classes during the growing season. The ETrF was lower early in the growing season for agricultural crops and gradually increased as the normalized difference vegetation index of crops increased, thus presenting more surface area over which water could transpire toward the mid-season. Comparison of predictions with Bowen ratio energy balance system measurements at Clay Center, NE, showed that METRIC™ performed well at the field scale for predicting evapotranspiration from a cornfield. If calibrated properly, the model could be a viable tool to estimate water use in managed ecosystems in subhumid climates at a large scale.

Key Words: energy balance, evapotranspiration, METRIC, SEBAL, water use

INTRODUCTION

Water is the most important constraint facing agriculture in most of the Central High Plains of the United States, including Nebraska. Nebraska's 8.2 million acres of irrigated lands are extremely vital to the state's economy. Local, state, and federal water management regulatory agencies need good-quality water-use estimates for different land surfaces to assess short- and long-term water management, planning, and allocations on a watershed scale. Evapotranspiration (ET) can be defined as the loss of water to the atmosphere from the ground, lake, pond, and vegetative surfaces due to vaporization of liquid water. Evapotranspiration is usually the largest hydrological flux through the summer months in the Great Plains. The ability to accurately estimate the magnitude of this flux will, therefore, go a long way toward computing the water balance and planning the use of available water resources. It is, however, the most difficult flux to quantify (Peacock and Hess 2004). Furthermore, quantification of this flux on a watershed or a regional scale is much more difficult than at a specific site. Evapotranspiration is highly dynamic in space and time because of the complex interaction of soil, vegetation, and climate. The Bowen ratio energy balance system (BREBS) and eddy correlation techniques offer alternatives for measuring surface energy fluxes, including evapotranspiration, at a footprint scale. Despite the high accuracy of techniques, they may not be practical when quantifying water use at regional scales due to the number of measurement sites needed and the operational expense of such a dense network.

Satellite remote sensing overcomes these issues with a broad spatial coverage and the potential exists for indirect evapotranspiration measurement. The land surface energy balance (EB) based models convert satellite sensed radiances into land surface characteristics to estimate evapotranspiration as a residual of the land surface energy balance equation. The Surface Energy Balance Algorithm for Land (SEBAL) was developed to quantify evapotranspiration over large areas using remote sensing-based land surface energy fluxes (Bastiaanssen et al. 1998a, 1998b).

The SEBAL model uses the near-surface temperature gradient (dT) between the land surface and air, estimated as an indexed function of radiometric surface temperature (T_s), thereby eliminating the need for absolutely accurate surface temperature (T_s) or air temperature (T_{air}) measurements to estimate sensible heat flux (H). The dT varies linearly with T_s, and this relationship is based on two anchor pixels (hot and cold pixels) where a value of H can be estimated. The maximum and minimum values of dT are calculated for the hot and cold pixels in an image and ultimately anchor H while preventing outliers in H estimation (Bastiaanssen et al. 1998a). The anchoring pixels can exist anywhere within the satellite image footprint. It was hypothesized that H at the cold pixel and latent heat flux (LE) at the hot pixel are zero. It follows that the evaporative fraction (EF) of the cold pixel equals one and that of the hot pixel equals zero. The EF (Λ) defines the partitioning of the surface EB by means of the latent heat flux (LE)/net available energy ($R_n - G$), with the net available energy ($R_n - G$) being defined as the difference in net radiation (R_n) and soil heat flux (G).

The SEBAL model is gaining global attention for its successful application worldwide. The model has been used to estimate riparian evapotranspiration (Goodrich et al. 2000), basinwide evapotranspiration (Tateishi and Ahn 1996), mapping regional runoff and precipitation (Church et al. 1995), developing crop coefficients (Bausch 1995; Tasumi et al. 2005a, 2005b; Singh and Irmak 2009) and for quantifying on-demand irrigation (Irmak and Kamble 2009). A critical issue with SEBAL is, however,

defining anchor pixels. When anchor pixels are not present on the imagery, assumptions may not hold, and then the SEBAL approach has been less than satisfactory (i.e., Singh et al. 2008).

To solve this dilemma, Allen et al. (2007a, 2007b) introduced the METRIC™ (Mapping Evapotranspiration at High Resolution using Internalized Calibration) model using similar principles to those of SEBAL, but with refinements to anchor pixels and various energy balance components. They introduced a better proxy for scaling satellite overpass time evaporation (EF) to 24-hour periods for the well-watered and fully vegetated areas of the image which represent the alfalfa-based reference evapotranspiration surface (ET_r). In METRIC™, LE at the cold pixel with full canopy cover (leaf area index [LAI] > 4) is taken as 1.05 ET_r, where ET_r is the alfalfa-based reference evapotranspiration. For the hot pixel, the LE estimate is based on a bare soil water balance using the FAO 56 approach (Allen et al. 1998).

METRIC™ estimates a so-called "fraction of reference ET (ETrF)" defined as the "ratio of instantaneous ET to the reference crop evapotranspiration (ET_r)" (Allen et al. 2007a, 2007b). The ETrF estimates from METRIC™ using remotely sensed data are instantaneous; even so, it allows estimating LE on a 24-hour basis. The daily reference crop evapotranspiration (ET_{r-24}) is multiplied with ETrF to estimate daily ET at each pixel of the Landsat scene. ETrF is similar to evaporative fraction used by Bastiaanssen et al. (1998a, 1998b). The instantaneous EF and ETrF are shown to be similar to the 24-hour EF and 24-hour ETrF, respectively (Shuttleworth et al. 1989; Verma et al. 1992; Brutsaert and Chen 1996; Trezza et al. 2003).

The demand for quantification of evapotranspiration over large areas is growing. Estimates based on satellite remote sensing offer a reasonable means for meeting this demand. The advantage of applying remote sensing–based evapotranspiration procedures is that the water used by the soil-water-vegetation system can be derived directly without the need to quantify other hydrological processes. Therefore, the remote sensing–based estimation of evapotranspiration has potential in quantification of large-scale water balances. The principal thrust of our study was to utilize the METRIC™ model to estimate water use in managed ecosystems in Great Plains environmental settings. In particular, we were interested in spatiotemporal distribution of the fraction of reference evapotranspiration (ETrF) on a regional scale. A total of eight Landsat 5 satellite images from 2005 and 2006 for path 29, row 32 were processed using METRIC™ algorithms.

MATERIAL AND METHODS

METRIC Model

Evapotranspiration estimation in METRIC™ is based on the principle of energy conservation. The model ignores minor energy components and considers only vertical fluxes (horizontal advective flux is not explicitly included) to estimate LE as a residual in the EB equation:

$$LE = R_n - G - H \quad (1)$$

where R_n is the net radiation, G is the soil heat flux, H is the sensible heat flux, and LE is the latent heat flux. The units for all the fluxes are in watts per meter square (W m^{-2}).

METRIC™ uses the empirical equation developed by Tasumi et al. (2003) to compute soil heat flux (G):

$$\frac{G}{R_n} = 0.05 + 0.18\, e^{-0.521LAI} \ (\text{if LAI} \geq 0.5)$$
$$\frac{G}{R_n} = (1.80\,(T_s - 272.15)/R_n + 0.084) \ (\text{if LAI} < 0.5) \quad (2)$$

where T_s (K) is the surface temperature determined from a satellite. Equation 2 suggests that when Leaf area index (LAI) is less than 0.5, the G/R_n ratio increases with higher rates of T_s and decreases with increasing LAI.

Using the aerodynamic function, sensible heat flux (H) is expressed as:

$$H = \frac{\rho \cdot C_p \cdot dT}{r_{ah}} \quad (3)$$

where ρ is the air density (kg m^{-3}), C_p is the specific heat of air (1004 Joules [J] per kilogram [kg^{-1}] per degree Kelvin [K^{-1}]), dT is the near-surface and air-temperature difference (K), and r_{ah} is the aerodynamic resistance to heat transfer (s m^{-1}) over the vertical distance.

METRIC™ uses two anchor pixels (hot and cold) where values of H can be estimated. The model does not require the actual absolute values of air temperatures (T_{air}) above each pixel, but only near-surface temperature difference (dT) to solve for H. The dT is used because of the difficulties in estimating surface temperature accurately from the satellite due to uncertainties in air temperature (T_{air}), atmospheric attenuation, contamination, and radiometric calibration of the sensor (Bastiaanssen et al. 1998a, 1998b; Allen et al. 2007a, 2007b). Use of dT between two heights above the surface allows for the calculation of only one value of r_{ah} from only one value of a second

aerodynamic roughness. The dT for each pixel is calculated as:

$$dT = T_{z1} - T_{z2} \quad (4)$$

where T_{z1} and T_{z2} are the air temperatures at height z1 (0.1 m) and z2 (2.0 m) for any particular pixel.

The dT is estimated assuming a linear relationship between dT and Ts that is calibrated to each satellite image to compensate for uncertainties in aerodynamic surface T_s and air temperature (T_{air}). The linearity assumption is based on the field research demonstrated by Wang et al. (1995), Bastiaanssen (1995), Franks and Beven (1997a, 1997b), and Franks and Beven (1999). If one can assume the presence of wet and dry pixels in the remotely sensed image, then the image-derived surface temperatures can be scaled to yield EF or ETrF ranging from 0 to 1. The basis of this assumption is that evaporative fluxes across a given domain may be bounded at the extremes, that is, no or nearly zero evaporation (hot or dry pixel) and potential evaporation (cold or wet pixel).

Estimation of Latent Heat Flux and Reference Evapotranspiration Fraction

The integration of LE over time in METRIC™ was split into two steps. The first step was to convert the instantaneous value of LE into daily ET_{24} values by holding the reference ET fraction constant (Allen et al. 2007a). An instantaneous value of ET (ET_{inst}) in equivalent evaporation depth is the ratio of LE to the latent heat of vaporization (λ):

$$ET_{inst} = 3600 \frac{LE}{\rho_w \lambda} \quad (5)$$

where 3600 is the time conversion from seconds to hours, and ρ_w is the water density (~1.0 Mg m^{-3}).

The reference ET fraction (ETrF) is defined as the ratio of instantaneous ET (ET_{inst}) for each pixel to the alfalfa-reference ET calculated using the standardized ASCE Penman-Monteith equation for alfalfa (ET_r) following the procedures given in ASCE-EWRI (2005):

$$ETrF = \frac{ET_{inst}}{ET_r} \quad (6)$$

ETrF serves as a surrogate for K_c (basal crop coefficient) and has been used with 24-hour ET_r in order to estimate the daily ET at each Landsat pixel:

$$ET_{24} = ET_rF \times ET_{r\text{-}24} \quad (7)$$

where ET_{24} is the daily value of actual ET (mm d^{-1}) and ET_{r-24} is 24-hour ET_r for the day of the image, calculated by summing hourly ET_r values over the day of image. The procedures outlined in ASCE-EWRI (2005) were used to calculate parameters in the hourly ET_r.

Although daily values of ET derived at the satellite overpass date are more helpful and practical, water regulatory agencies are interested in seasonal ET estimates to assess water management, planning, and allocation. First, to obtain seasonal ET, the reference ET fraction (ETrF) for each satellite overpass date is calculated for the considered period. The ETrF is then interpolated (i.e., linear, cubic spline) for other dates between the dates of satellite overpasses. Subsequently, the interpolated ETrF is multiplied with the corresponding calculated ET_{r-24} to obtain actual ET (ET_{24}) for the dates between satellite overpasses. Seasonal ET can be obtained by summing daily ET_{24} values for the considered period.

METRIC Model Setup

The METRIC™ model calculates actual evapotranspiration by utilizing satellite images containing both shortwave and thermal bands. The sensible heat (H) for each pixel of an image is estimated at each pixel, and equation 1 is used to find LE. Values for H are calculated across an image according to the surface temperature (T_s). This is done using a "dT vs. T_s" function. The dT can be estimated as a linear function of surface temperature (Bastiaanssen et al. 1998a). It is the difference between the air temperature very near the surface, at 0.1 m above the zero plane displacement height, d, and the air temperature at 2 m above the zero plane displacement height.

The linear equation for dT vs. T_s in METRIC™ is developed by using the dT values for the cold and hot pixels, which provide internal and automatic calibration. In addition, internal calibration of the EB utilizes ground-based reference ET (ET_r) to tie down the derived EB (Allen et al. 2007a, 2007b). Therefore, use of quality controlled hourly ET_r is important to improve accuracy of daily and longer period ET estimates.

In METRIC™, cold and hot pixels should be located near the weather station (~within 50 km). The cold pixel is used to define the amount of ET occurring from the well-watered and fully vegetated areas of the image, which represent instances where the maximum (or near maximum) amount of available energy is being consumed by evaporation. For this study, we selected a number of cold pixel candidates for each image representing an agricultural area under a center pivot irrigation

system that has vegetation at full cover (LAI is usually greater than 4.0 m^2) to estimate ET at the cold pixel. We assumed that ET = 1.05 ET_r at the cold pixel. The ET_r is the rate of ET from the alfalfa reference calculated using the ASCE Standardized Penman-Monteith equation for alfalfa. H for the cold pixel was then calculated as $H = R_n - G - 1.05\ ET_r$.

The selection of the hot pixel follows the same procedure as for the cold pixel. The hot pixel should be located in a dry and bare agricultural field where one can assume evaporative flux is 0. We selected the hot pixel candidates with a surface albedo similar to dry and bare fields (0.175-0.2) with very low LAI (usually less than 0.1). In south-central Nebraska, we found that the hot pixels could not be assumed to have zero evaporation because of high frequency of rain in the region. Therefore, H was estimated as $R_n - G - ET_{bare\ soil}$, where $ET_{bare\ soil}$ was obtained by running a daily soil water balance model of the surface soil using ground-based weather measurements (Allen et al. 1998). The METRIC™ model was then run for each of the cold and hot pixel candidates. The best suitable anchor pixels were determined based on the distribution of ETrF over the image. For instance, ETrF of well-irrigated and fully vegetated agricultural crops should have an ETrF of 1.0, on average.

Landsat Satellite Datasets and Processing

Landsat 5 (LT5) cloud-free, systematic terrain-corrected (Level 1T) satellite images (path 29, row 32) were obtained from the Earth Explorer, USGS site (http://www.edcsns17.cr.usgs.gov/EarthExplorer/) for the 2005 and 2006 growing season. The acquisition dates for Landsat 5 images were May 19, June 20, August 7, and September 8, 2005, while the dates for 2006 were May 22, June 23, July 25, and October 13. These images had a cloud cover of less than 10%. The METRIC™ algorithms developed by University of Idaho (Allen et al. 2007a, 2007b) were adapted and modified in Erdas Imagine® Image Processing Software (Leica Geosystems Geospatial Imaging, LLC) to achieve the objectives.

The seasonal progression of land surface conditions were characterized with a normalized difference vegetation index (NDVI). The index was computed using reflectance for the near infrared (ρ_{NIR}) and red (ρ_{RED}) bands:

$$NDVI = \frac{\rho_{NIR} - \rho_{RED}}{\rho_{NIR} + \rho_{RED}} \quad (8)$$

Experimental Setup Description for the Study Area

The field data were collected at the University of Nebraska–Lincoln South Central Agricultural Laboratory near Clay Center, NE (40°34′N, 98°08′W; elevation 552 m). The Pioneer 33B51 corn hybrid was planted for the years 2005 and 2006 at 0.76 m row spacing and a seeding density of approximately 73,000 seeds/ha and with planting depth of 0.05 m. The Pioneer 33B51 hybrid had a comparative relative maturity of 113 to 114 days. In 2005 corn was planted on April 22, emerged on May 12, reached full canopy closure on July 4, reached silking stage on July 12, matured on September 7, and was harvested on October 17. In 2006 corn was planted on May 12, emerged on May 20, reached complete canopy closure on July 8, reached silking stage on July 15, matured on September 13, and was harvested on October 5.

The soil at the experimental site is Hastings silt loam, which is a well-drained soil on uplands. It is a fine, *montmorillonitic, mesic Udic Argiustoll*, with field capacity of 0.34 $m^3\ m^{-3}$ and permanent wilting point of 0.14 $m^3\ m^{-3}$. The particle size distribution is 15% sand, 62.5% silt, and 20% clay. The soil has a 2.5% organic matter content. The experimental field (13 ha) was irrigated using a subsurface drip irrigation system. The drip laterals were spaced every 1.52 m (in the middle of every other crop row) and were installed at a depth of approximately 0.4 m from the soil surface. Irrigation was applied twice or three times a week to replenish the soil water content to approximately 90% of the field capacity in the top 0.90 m of the soil profile, which was considered to be the effective root-zone depth for corn. Detailed description of experimental field data collection methods were reported by Irmak and Irmak (2008) and Irmak et al. (2008).

Flux Measurements Using a Bowen Ratio Energy Balance System

This study used the surface energy balance flux data that were measured and reported by Irmak and Irmak (2008) and Irmak et al. (2008). The BREBS was installed in the middle of the experimental field with a fetch distance of 260 m in a north-south direction and 137 m in an east-west direction. The row orientation of the field was in an east-west direction. There were adequate fetch conditions since the prevailing wind direction in the experimental site is usually from the south during the spring and summer months. In addition, the experimental field was surrounded with large irrigated cornfields in four

directions. The BREBS measurement heights were thus considered to be within the boundary layer over the irrigated cornfield. The BREBS measurements were made daily for 2005 and 2006.

Measurements were made using a deluxe version of a BREBS (Radiation and Energy Balance Systems, REBS, Inc., Bellevue, WA). The chromel-constantan thermocouple air temperature and relative humidity (RH) probes (Model THP04015 for temperature, and THP04016 for RH; REBS, Inc., Bellevue, WA) were used to measure air temperature and RH gradients. The BREBS used an automatic exchange mechanism that physically exchanged the temperature and RH sensors at two heights above the canopy. Soil heat flux was measured using three REBS HFT-3.1 heat flux plates and three soil thermocouples. Each soil heat flux plate was placed at a depth of 0.08 m below the soil surface approximately 45 cm apart from each other. Three REBS STP-1 soil thermocouple probes were installed a few centimeters from each soil heat flux plate. Measured soil heat flux values were adjusted to soil temperature and soil water content as measured using three REBS SMP1R soil moisture probes at a depth of 0.06 m. The three sets of soil heat flux, soil temperature, and soil water content probes were installed on the crop row on the ridge, in the middle of the dry furrow where the drip lateral pipe was not present, and in the middle of the furrow where the drip lateral pipe was present (the drip laterals were installed on every other crop row in the middle of the furrow). The average soil heat flux values from three sensors were used in the calculations.

R_n was measured using a REBS Q-7.1 net radiometer installed approximately 4.5 m above the soil surface. Shortwave radiation and longwave radiation were measured simultaneously using a model REBS THRDS7.1 double-sided total hemispherical radiometer, and the hourly albedo values were calculated from the ratio of outgoing shortwave to incoming shortwave radiation. Wind speed and direction at 3 m height were monitored using a Model 034B cup anemometer (Met One Instruments, Grant Pass, OR) that had a wind speed range of 0-44.7 m s^{-1} with a starting threshold of 0.28 m s^{-1}. All variables were sampled at 30 s intervals and averaged and recorded every hour for energy balance calculations using a Model CR10X datalogger and AM416 Relay Multiplexer (Campbell Scientific, Inc., Logan, UT). The satellite overpasses on path 29, row 32, were usually between 11:00 a.m. to 11:10 a.m. Central Standard Time. The hourly BREBS measurements from 11:00 a.m. and 12:00 p.m. Central Standard Time were converted to represent the instantaneous fluxes for each satellite overpass date. Details of flux measurements were given by Irmak and Irmak (2008) and Irmak et al. (2008).

Meteorological Data

Weather data were acquired from the High Plains Regional Climate Center's (HPRCC) Automated Weather Data Network (AWDN). The AWDN stations record hourly data for air temperature, humidity, soil temperature, wind speed and direction, solar radiation, and precipitation. Reference ET (ET_r) values were calculated using the ASCE-EWRI (2005) standardized Penman-Monteith equation for alfalfa reference. Table 1 shows average weather conditions at South Central Agricultural Laboratory measured with BREBS for the days of Landsat overpass for 2005 and 2006 growing seasons.

RESULTS AND DISCUSSION

Mapping Spatiotemporal Distribution of Normalized Difference Vegetation Index, Available Energy, and Reference Evapotranspiration

Figure 1 shows land-use classes for path 29 and row 32. The land-use classes for a given scene have different surface roughness characteristics because of the height and density of land surface properties. Therefore, use of a land-use map in METRIC might improve parameterization of the surface roughness parameter especially if a high level of accuracy and detail are represented in the land-use map for the study area. The land-use map was developed at the Center for Advanced Land Management Information Technologies (CALMIT) using level 1T LT5 scenes for 2005 (CALMIT 2006). The scale of the map is 1:100,000 with a ground resolution of 28.5 m. There are 25 land-use classes, and agricultural crops are identified as either irrigated or dryland. The overall accuracy of the statewide classification was calculated at 80.43%. The top portion of Figure 1 covers south-central Nebraska and includes primarily agricultural crops such as corn and soybeans with some grain sorghum. Pasture (rangeland, grassland) and native vegetation are located from west to east in southern Nebraska and cover as much as one-third of the Nebraska portion of the scene. The Kansas portion, one-quarter portion of scene, includes mainly small grains (wheat) and rangeland.

To quantify the spatial distribution of seasonal ET, at least one image per month was required for an accurate and continuous characterization of the ETrF (fraction of

TABLE 1
AVERAGE WEATHER VARIABLES AT THE SOUTH CENTRAL AGRICULTURAL LABORATORY NEAR CLAY CENTER, NEBRASKA, FOR THE DAYS OF LANDSAT OVERPASS FOR 2005 AND 2006 GROWING SEASON

Date	T_{max} (°C)	T_{min} (°C)	RH_{max} (%)	RH_{min} (%)	U_3 (m s^{-1})	R_s (W m^{-2})	ET_r (mm d^{-1})	$LE/(R_n - G)^*$
May 19, 2005	30.7	10.8	84.4	22.3	3.20	342.6	9.62	0.42
June 20, 2005	33.0	18.9	96.2	47.8	4.10	315.5	8.22	0.94
August 7, 2005	31.4	16.2	97.3	51.2	3.10	257.5	5.56	0.98
September 8, 2005**	**30.5**	**18.2**	**96.1**	**53.3**	**3.58**	**242.7**	**5.24**	**1.45***
May 22, 2006	29.5	13.9	80.7	40.5	4.40	271.1	8.09	0.19
June 23, 2006	28.4	15.1	98.3	40.5	2.02	332.9	7.29	0.80
July 25, 2006*	**32.6**	**21.2**	**90.7**	**51.3**	**4.65**	**246.7**	**6.84**	**1.14***
October 13, 2006	11.9	-2.9	79.5	20.0	5.48	198.5	3.99	0.44

Notes: The climate variables are T_{max} = maximum air temperature, T_{min} = minimum air temperature, RH_{max} = maximum relative humidity, RH_{min} = minimum relative humidity, U_3 = wind speed at 3 m height, R_s = incoming shortwave radiation, and ET_r = reference evapotranspiration. All the climate variables were from Bowen ratio energy balance system except the ET_r data, which were calculated using the standardized ASCE Penman-Monteith equation for alfalfa following the procedures given in ASCE-EWRI (2005) with the data from the High Plains Regional Climate Center weather station located near the study field.
*Partitioning of $R_n - G$ to LE at the satellite day.
**Advection occurred.

reference ET or relative ET) curve for each Landsat pixel for the growing period (May 1–October 15). Only four Landsat 5 images were selected from May 19 through September 8 in 2005 to demonstrate progression of vegetation growth and corresponding fluxes on a spatial scale in the study domain. Figure 2 shows the progression of NDVI on May 19, June 20, August 7, and September 8 during the 2005 growing season while Figure 3 shows $R_n - G$ for the same days, respectively. NDVI is a measure of vegetation amount and condition and associated with biomass, leaf area index, and percentage of vegetation cover. It can provide information about the crop stand, crop development stage, crop conditions, and water stress conditions. $R_n - G$ shows the amount of available energy for latent heat (LE) and sensible heat (H).

The NDVI values were usually lower for agricultural lands (top portion of the image in Fig. 2) than rangeland/natural vegetation (bottom portion of Fig. 2). NDVI values were around 0.2–0.3 for agricultural crops on May 19, while they were as high as 0.6 for rangeland/natural vegetation. The NDVI increased gradually during the vegetative development stage of agricultural crops (May through June) and reached its maximum value (~0.75 and 0.85) in August. It remained fairly constant during the reproductive stage of crops (August through September).

Similar to NDVI progression, the available energy ($R_n - G$) increased with the crop growth and development (Fig. 3). This increase in $R_n - G$ is due to the increase in the vegetative ground cover. Higher ground cover as indicated by higher NDVI acts as a barrier to the conduction of solar radiation to the soil surface so that less R_n is consumed in heating of the soil (G). Results showed that $R_n - G$ was lower when much of ground was bare soil ranging from 450 W m^{-2} to 480 W m^{-2} and higher (550-600 W m^{-2}) when NDVI was high.

Figure 4A shows the ETrF for the LT5 satellite overpass on May 19, 2005, for path 29, row 32. As expected, the ETrF was highly variable in south-central Nebraska due to variation in soil, cropping practices, and vegetation development. The ETrF values were usually lower for agricultural lands than rangeland/natural vegetation in May. This was due to crop germination and emergence stages at this time. The grazed rangeland/natural vegetation has green vegetation in May as evidenced by

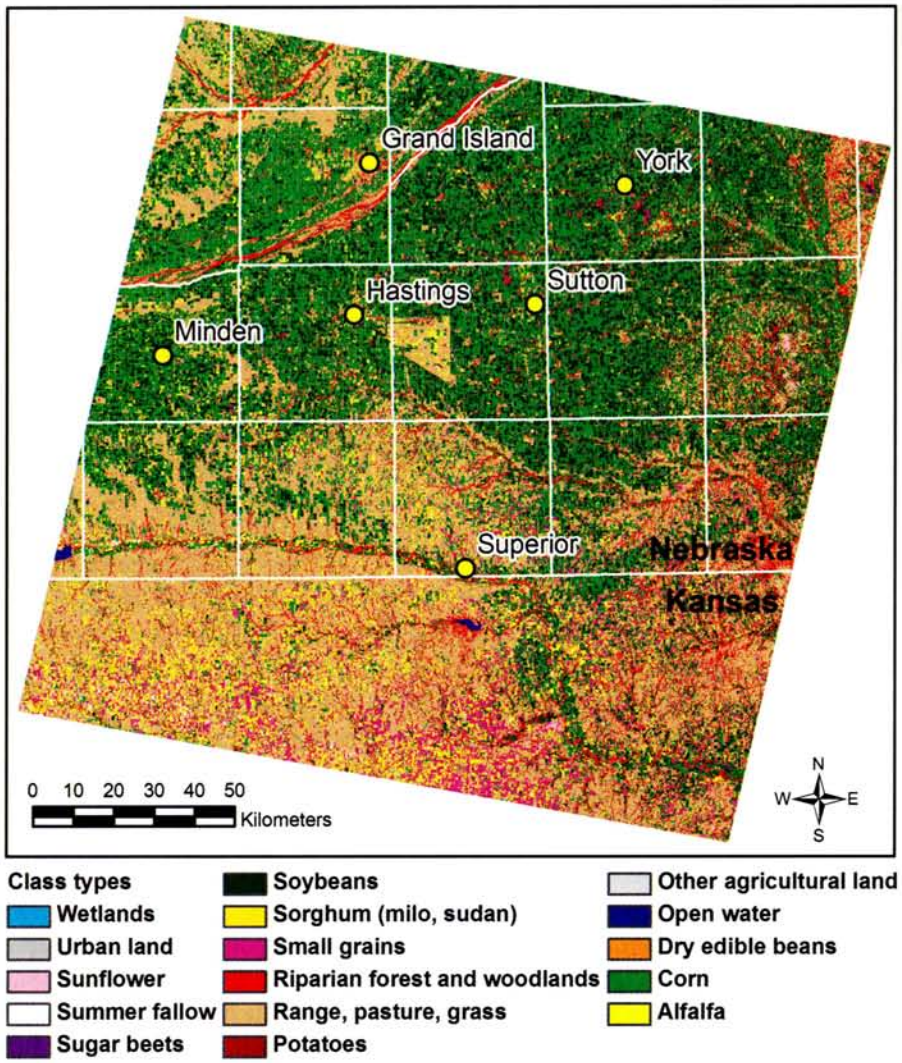

Figure 1. Land-use map of the study area (path 29, row 32) originated from 2005 Nebraska land-use map.

higher NDVI values in the scene. The corresponding ETrF values from grazed rangeland/natural vegetation pixels were quite high in May, indicating that grazed rangeland/natural vegetation is transpiring at near potential rates and most of the $R_n - G$ was used for transpiration. Daily ETrF values on May 19, 2005, were from 0.3 to 0.4 for agricultural lands and was as high as 0.9 for the natural vegetation/rangeland represented in the image (Fig. 4A).

The ETrF vales for agricultural crops generally increased on the June image (Fig. 4B) and were from 0.6 to as high as 0.9. Most of the spatial variability in ETrF was probably due to variation in management practices mainly cropping practices (soybean or corn), soil moisture, hybrids, and dates of planting for agricultural fields. Figure 4C shows the ETrF distribution on August 7, 2005. The ETrF from agricultural land was much higher (around 1.0 or higher) than the natural vegetation/rangeland. By the end of July agricultural crops usually reach their full canopy cover and vegetative development stops. This is demonstrated by a high NDVI for agricultural crops in August, which indicates a maximum leaf area index (Fig. 2C). At this stage, well-watered crops usually transpire at their potential rates (potential ET). The agricultural crops in south-central Nebraska are irrigated with center pivot irrigation systems to supplement additional water from mid-June to mid-September and to prevent crop water stress conditions. However, most of the rangeland is not irrigated, and could now be suffering water stress consistent with lower ETrF.

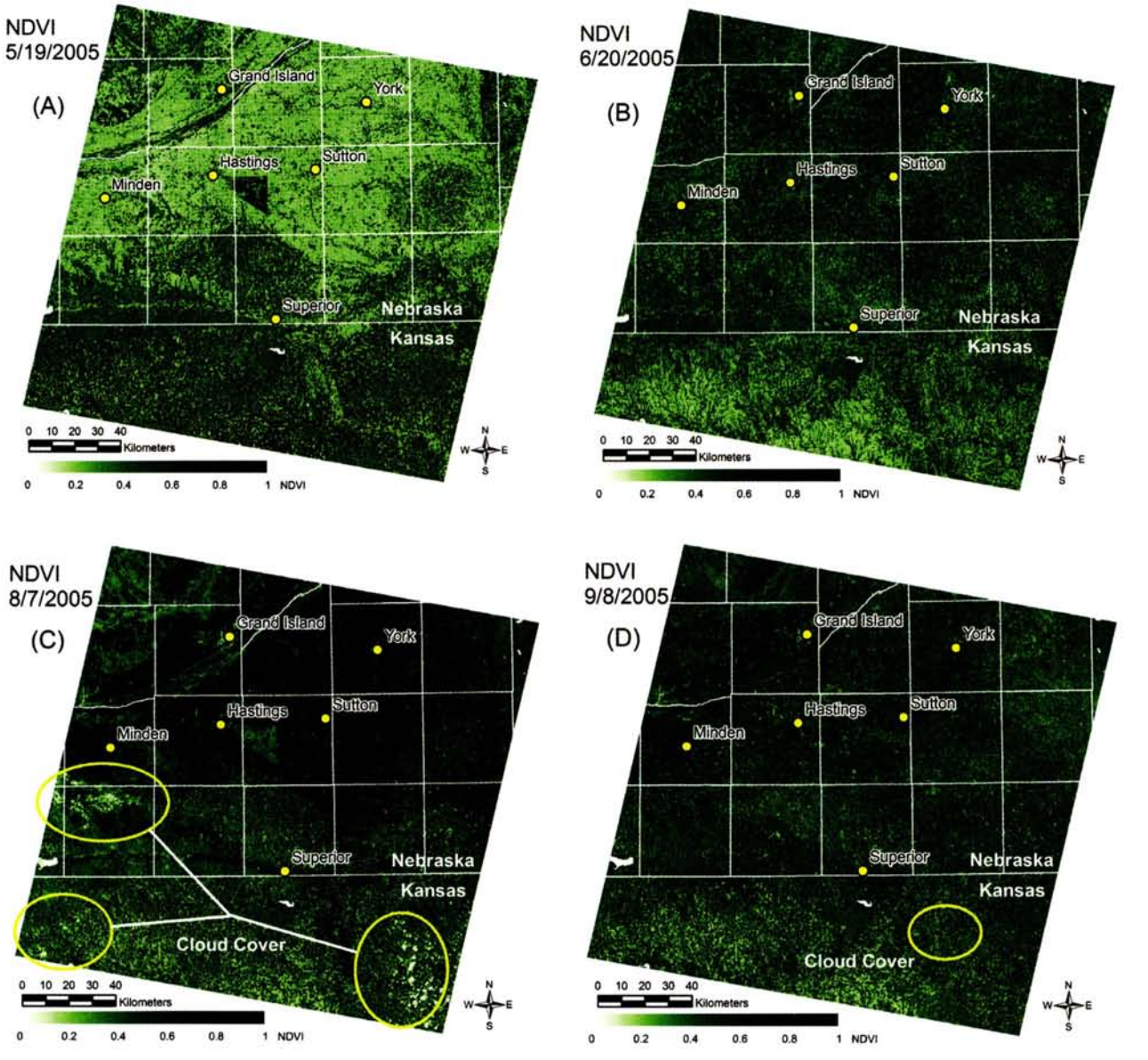

Figure 2. Landsat-derived normalized difference vegetation index (NDVI) values for path 29, row 32 on (A) May 19, 2005; (B) June 20, 2005; (C) August 7, 2005; and (D) September 8, 2005. Cloud cover is identified by yellow circles in the August 7 and September 8 images.

There was an obvious increase in ETrF for agricultural crops in the September 8 image compared to values in August 8. The ETrF values were around 1.0 and 1.1, indicating that actual evapotranspiration by agricultural crops is equal to potential ET. These values were slightly higher than expected. Higher ETrF on September 8 could be attributed to the high amount of precipitation that was received at most of the weather stations on the Landsat scene prior to the satellite pass on September 5. The ET_rF of the hot pixel was 0.94 on September 8, determined by solving the daily surface-layer water-balance model of FAO-56 (Allen et al. 1998). This indicates a significant residual evaporation at the hot pixel. Similar results were found by Singh et al. (2008), who applied SEBAL model for the same dataset.

The ETrF maps generated by the METRIC™ model showed the spatial and temporal distribution of relative ET during the growing season as land surface conditions continuously changed (Fig. 4). The information also allowed us to follow the seasonal trend in ETrF for major land-use classes on the image. The ETrF was lower early in the growing season for agricultural crops and gradually

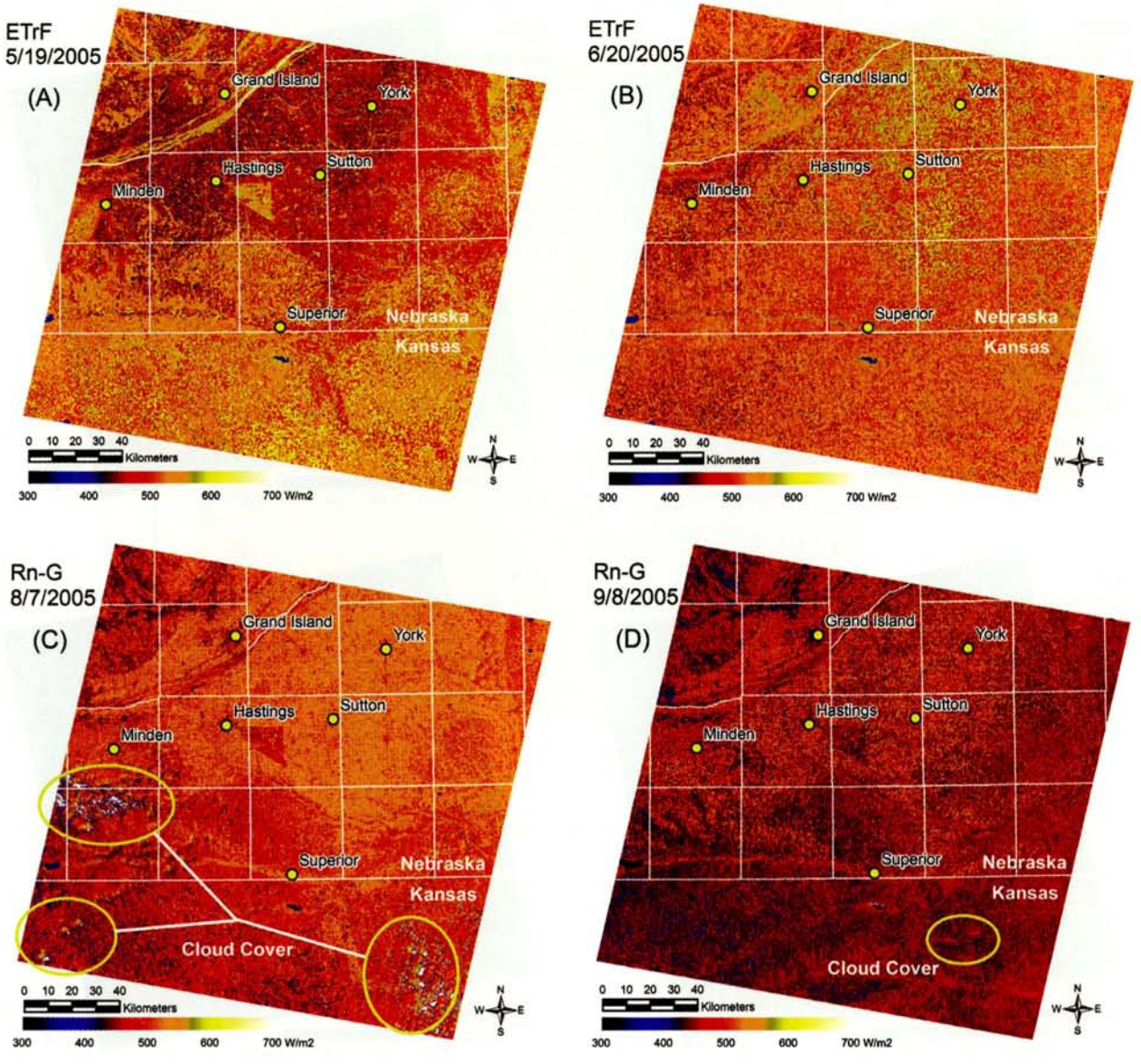

Figure 3. Landsat derived available energy (R_n – G) values used for path 29, row 32 on (A) May 19, 2005; (B) June 20, 2005; (C) August 7, 2005; and (D) September 8, 2005. Cloud cover is identified by yellow circles in the August 7 and September 8 images.

increased as the agricultural crops increasingly transpire water toward the midseason.

ETrF from SEBAL and METRIC™ models has been used to serve as a surrogate for K_c (basal crop coefficient) in order to estimate the daily ET from a satellite. Singh and Irmak (2009) developed locally calibrated ET_r-based K_c curves for corn (*Zea mays* L.), soybeans (*Glycine max* L.), sorghum (*Sorghum bicolor* L. Moench), and alfalfa (*Medicago sativa* L.) grown under irrigated and dryland conditions in Nebraska's climate. The results indicated that single K_c data sets typically derived for specific crop varieties for the region would lead to substantial error(s) in ET_c calculation. Similar work was done by Tasumi et al. (2005a) using ET maps created by SEBAL model. They developed the distribution of K_c curves for a large number of individual fields by crop type (alfalfa, bean, corn, peas, potato, sugar beet, spring wheat, and winter wheat in south-central Idaho. Both studies (Singh and Irmak 2009; Tasumi et al. 2005a) further developed the relationship between K_c curves and vegetation indices such as NDVI in order to obtain more rapid and simple estimates of ET based solely on the vegetation index, NDVI.

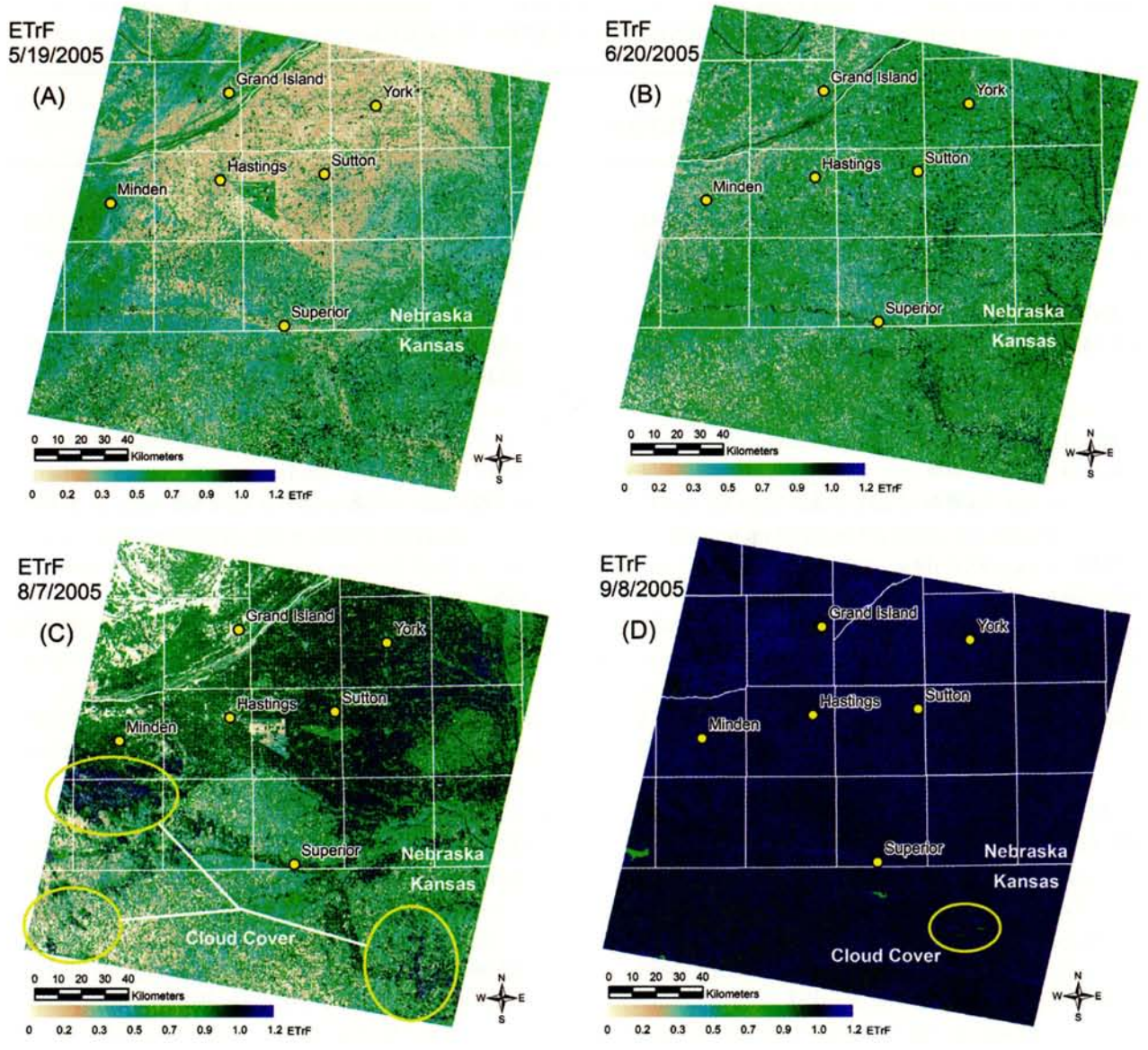

Figure 4. Landsat derived ETrF values (reference evapotranspiration fraction) for path 29, row 32 on (A) May 19, 2005; (B) June 20, 2005; (c) August 7, 2005; and (D) September 8, 2005. Cloud cover is identified by yellow circles in the August 7 and September 8 images.

Evaluation of the METRIC™ for Estimating Energy Fluxes and Daily Evapotranspiration

The comparisons of measured and METRIC™-estimated instantaneous incoming and outgoing radiation fluxes for 2005 and 2006 are presented in Table 2. The model estimated incoming solar radiation ($R_s\downarrow$) well for both years with root mean square of error (RMSE) of less than 20 watts per meter squared (W m^{-2}). The slope of regression coefficients was close to unity indicating a very strong fit and little systematic bias between estimated and measured incoming radiant energy flux. On average, BREBS-measured $R_s\downarrow$ was 821 W m^{-2} for the combined dataset (2005 and 2006).

Table 1 shows average weather variables at the South Central Agricultural Laboratory near Clay Center, NE, for the days of Landsat overpasses for the 2005 growing season. The climate variables are T_{max} = maximum air temperature (°C), T_{min} = minimum air temperature (°C), RH_{max} = maximum relative humidity (%), RH_{min} = minimum relative humidity, U_3 = wind speed at 3 m height (m s^{-1}), R_s = incoming shortwave radiation (W m^{-2}), and ET_r =

TABLE 2
EVALUATION OF METRIC™ MODEL

Fluxes (units)	Year	BREBS	METRIC	Slope	RMSE	Percentage error	r^2
Rs↓ (W m2)	2005	849	841	0.989	12.9	1.5	0.872
	2006	807	829	1.030	17.9	2.2	0.957
Rs↑ (W m2)	2005	117	148	1.268	15.5	13.2	0.825
	2006	112	149	1.339	20.9	18.8	0.547
R1↓ (W m2)	2005	417	373	0.889	27.0	6.5	0.210
	2006	371	355	0.940	29.8	8.0	0.198
R1↑ (W m2)	2005	523	474	0.871	49.7	9.5	0.594
	2006	525	451	0.857	39.3	7.5	0.825
Rn (W m2)	2005	571	575	1.004	12.7	2.2	0.840
	2006	529	530	1.002	27.6	5.2	0.683
G (W m2)	2005	62	72	0.8991	9.4	15.0	0.667
	2006	60	73	1.254	12.1	21.6	0.463
H (W m2)	2005	122	130	0.886	46.5	38.2	0.393
	2006	193	245	1.251	31.5	16.4	0.990
LE (W m2)	2005	442	373	0.842	34.100	7.7	0.988
	2006	280	212	0.845	36.818	13.2	0.982
ETrF	2005	0.88	0.818	0.912	0.060	6.8	0.882
	2006	0.52	0.463	0.937	0.058	11.2	0.898
ETc (mm d-1)	2005	5.690	5.857	1.057	0.348	4.3	0.918
	2006	5.028	5.179	0.973	0.257	4.2	0.960

Notes: Instantaneous incoming shortwave (Rs↓), outgoing shortwave (Rs↑), incoming longwave (Rl↓), outgoing long wave (Rl↑) radiation fluxes, net radiation (Rn), soil heat flux (G), sensible heat flux (H), and latent heat flux (LE) at the BREBS flux-tower footprint at South Central Agricultural Laboratory for 2005 and 2006. BREBS-measured and METRIC predicted average flux for each year is also included. Statistics include slope of regression line (with intercept forced to zero), root mean square of error (RMSE), percentage error (RMSE/mean flux), and r^2 of the regression line between BREBS-measured and METRIC™-predicted values.

reference ET (mm d^{-1}). All the climate variables were from the BREBS except the ET_r, which was calculated using the standardized ASCE Penman-Monteith equation for alfalfa following the procedures given in ASCE-EWRI (2005) with the data from the HPRCC weather station located near the study field. The partitioning of available energy ($R_n - G$) to latent heat (LE) calculation for each satellite date is shown in the last column. If $LE/(R_n - G)$ is greater than 1.0, this indicates advection on that day. In this case H represents the movement of energy from the air to the canopy so that LE can exceed $R_n - G$. The higher the number, the higher the contribution of advection. BREBS data indicated that there was strong advection on September 8, 2005 ($LE/(R_n - G) = 1.45$) of the Landsat overpass days, thus, heat was transferred to the cropland area, creating additional energy to be used by the crop to meet the high ET demand on that day. This was expected since there was a large nonirrigated grassland area surrounding the experimental field at South Central Agricultural Laboratory that acted as a source for advective heat. Daily ET_r in September and October was the lowest among the satellite overpass dates for both years (Table 1).

Table 2 shows estimates of instantaneous incoming shortwave ($R_s\downarrow$), outgoing shortwave ($R_s\uparrow$), incoming longwave ($R_l\downarrow$) and outgoing longwave ($R_l\uparrow$) radiation fluxes, net radiation (R_n), soil heat flux (G), sensible heat flux (H), and latent heat flux (LE) at the BREBS flux-tower footprint at South Central Agricultural Laboratory for 2005 and 2006. Statistics include the RMSE, percentage error (RMSE/mean flux), and r^2 of the regression line between BREBS-measured and METRIC™-estimated values. The outgoing shortwave radiation ($R_s\uparrow$) was calculated by multiplying albedo with $R_s\downarrow$. On average, BREBS-measured $R_s\uparrow$ for the two-year dataset was 114 W m^{-2}, indicating that approximately 14% of incoming solar radiation ($R_s\downarrow$) was reflected back ($R_s\uparrow$) to the atmosphere (Table 2). METRIC™ estimated R_n well for both years. The statistics of R_n values of our study are comparable with those observed by other researchers (Crawford and Duchon 1999; Diak et al. 2000; Jacobs et al. 2004; Singh et al., 2008).

METRIC™ overestimated sensible heat flux (H) by 17% with a RMSE of 31.5 W m^{-2} in 2006. The model poorly estimated H for the September 8 image in 2005. Poor estimation of H on this date was due to a recent precipitation event. Precipitation occurring prior to the Landsat image date created wet surface conditions where LE was greater than zero for all potential hot pixel candidates.

There was a good fit between METRIC™ estimated and BREBS-measured ET_rF for 2005 and 2006 as evidenced by high r^2 values (Table 2; Fig. 5). Both METRIC™ and BREBS measurements demonstrated that very high ETrF was obtained for the days that advection occurred in the experimental field. The ETrF for the two advective dates are shown inside circles on Figure 5. We should note that BREBS-measured ET_rF was calculated by dividing daily values of BREBS-measured ET (mm) to daily reference ET (ET_r). However, METRIC values were obtained by dividing instantaneous ET (ET_{inst}) to daily ET_r, and extended to the full day as a constant in order to obtain daily ET for each satellite overpass date.

METRIC™ ET compared well with observations for both years as evidenced by high r^2 and low RMSE values (Fig. 6; Table 2). The RMSE was less than 0.5 mm on a daily basis for both years. The lowest ET was measured prior to harvest on October 13, 2006. The largest discrepancy in ET was on this date, with 0.88 mm underestimation by METRIC™. Overall, our validation analysis results showed that METRIC™ performed well at the field scale for estimating ET from a cornfield. Results also showed that the daily ET estimates were much closer to the measured ET than estimates of H and G fluxes to measured H and G fluxes.

CONCLUSION

In Nebraska, surface water is regulated by the Nebraska Department of Natural Resources (NDNR) and groundwater is regulated by the 23 Natural Resources Districts (NRDs). According to NDNR, water demands meet or exceed supply limits in many basins, and NDNR has designated these basins as fully appropriated or overappropriated. The dilemma for management entities is how to maintain profitable agricultural operations that are dependent on irrigation water while protecting surface water and groundwater resources to comply with water compacts or basinwide water management goals. Nebraska is presently engaged in a water planning process in which even small errors could have serious impacts over the long term. If ET is over- or underestimated, some river basins may be needlessly closed or mistakenly left open to further development. Clearly, Nebraska has many economic factors at stake in water planning and management decisions. There is a need to develop scientifically sound methods that provide reliable assessment of water management policies.

The METRIC™ is a hybrid model that combines remotely sensed energy balance via satellite data and

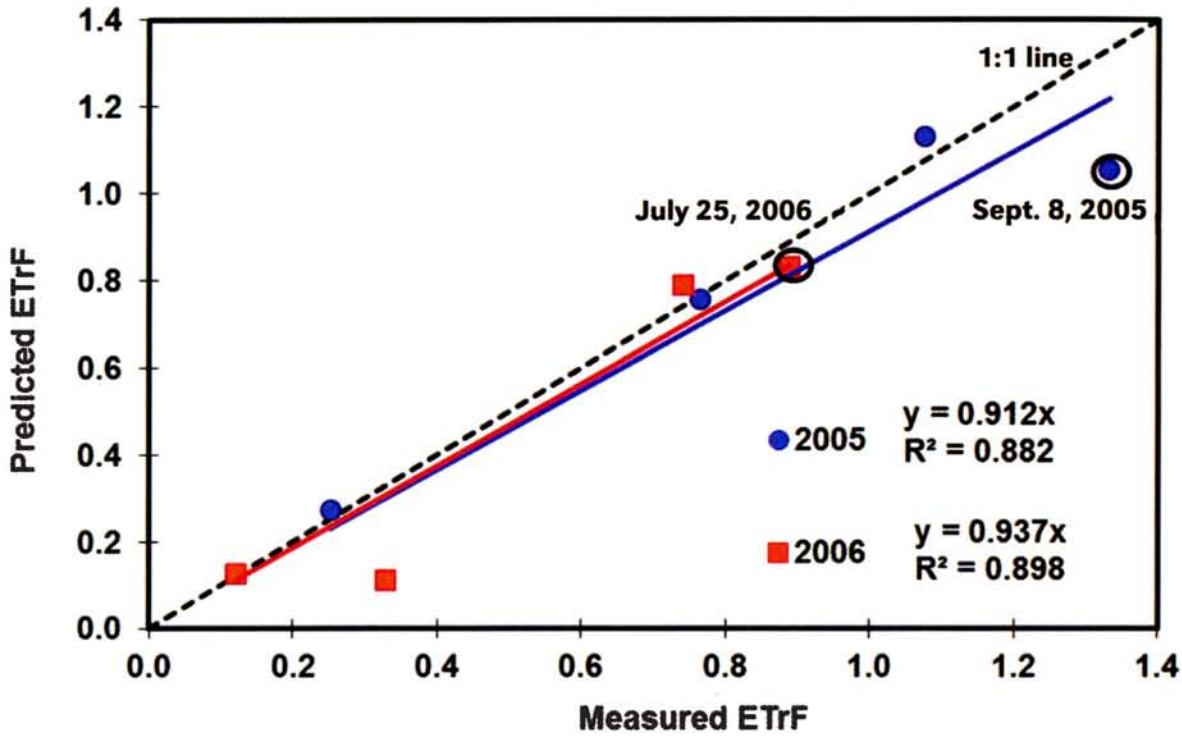

Figure 5. BREBS-measured and METRIC™-estimated evaporative fraction (ETrF) at the BREBS flux-tower footprint at South Central Agricultural Laboratory. The ETrF for the two advective dates are shown inside circles.

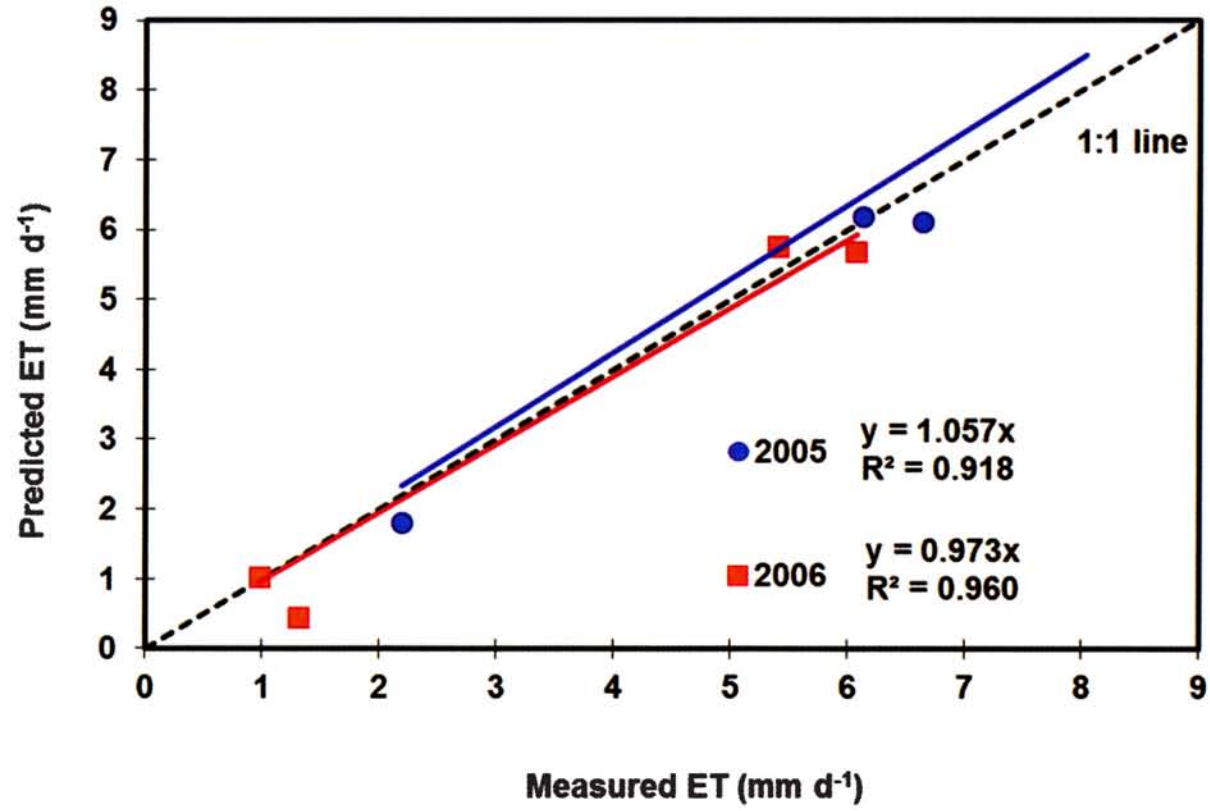

Figure 6. BREBS-measured and METRIC™-estimated daily evapotranspiration (ET, mm d^{-1}) at the BREBS flux-tower footprint at South Central Agricultural Laboratory.

ground-based evapotranspiration via in situ meteorological measurements in order to determine evapotranspiration. The application of the model gave an insight into the spatiotemporal distribution of relative ET on a landscape scale (170 × 183 km area). If calibrated properly, the model could be a viable tool to estimate water use in managed ecosystems in subhumid climates on a large scale, and particularly to assess short- and long-term water management, planning, and allocations. However, there are a few constraints with application of the model to create monthly and seasonal ET maps. Currently, a number of efforts are being made at the University of Nebraska–Lincoln to use METRIC™ in agricultural water management. Some of the efforts include (1) calibrating model algorithms against measurements over different vegetation, climate, and water regimes in the Great Plains; (2) testing submodels to estimate H, G, LAI, and other variables under various land surfaces and developing improved algorithms (or localized calibration of the model) if needed; (3) validating the model in the advective conditions; (4) developing a GIS-based soil water model to account for background evaporation; (5) automating hot and cold pixel selection; and (6) comparing pixel-by-pixel values with other remote sensing–based models.

ACKNOWLEDGMENTS

The authors acknowledge METRIC™ development and training provided by the University of Idaho and the research collaboration with the University of Idaho Kimberly Research and Extension Center during 2007–2010.

REFERENCES

Allen, R.G., L.S. Pereira, D. Raes, and D.M. Smith. 1998. *Crop Evapotranspiration: Guidelines for Computing Crop Water* Requirements. FAO Irrigation and Drainage Paper No. 56. Food and Agriculture Organization of the United Nations, Rome, Italy.

Allen, R.G., M. Tasumi, A. Morse, R. Trezza, J.L. Wright, W.G.M. Bastiaanssen, W. Kramber, I. Lorite, and C.W. Robison. 2007a. Satellite-based energy balance for mapping evapotranspiration with internalized calibration (METRIC): Applications. *Irrigation and Drainage Engineering* 133:395–406.

Allen, R.G., M. Tasumi, and R. Trezza. 2007b. Satellite-based energy balance for mapping evapotranspiration with internalized calibration (METRIC): Model. *Journal of Irrigation and Drainage Engineering* 133:380–94.

ASCE-EWRI. 2005. *The ASCE Standardized Reference Evapotranspiration Equation*, ed. R.G. Allen, I.A. Walter, R.L. Elliot, T.A. Howell, D. Itenfisu, M.E. Jensen, and R.L. Snyder. Environmental and Water Resources Institute of the American Society of Civil Engineers. ASCE Standardization of Reference Evapotranspiration Task Committee Final Report, ASCE, Reston, VA.

Bastiaanssen, W.G.M. 1995. Regionalization of surface flux densities and moisture indicators in composite terrain: A remote sensing approach under clear skies conditions in Mediterranean climates. Ph.D. diss., Wageningen Agricultural University, Netherlands.

Bastiaanssen, W.G.M., M. Menenti, R.A. Feddes, and A.A.M. Holtslag. 1998a. A remote sensing surface energy balance algorithm for land (SEBAL): 1. Formulation. *Journal of Hydrology* 212–213:198–212.

Bastiaanssen, W.G.M., H. Pelgrum, J. Wang, Y. Ma, J. Moreno, G.J. Roerink, and T. Van der Wal. 1998b. A remote sensing surface energy balance algorithm for land (SEBAL): 2. Validation. *Journal of Hydrology* 212–213:213–29.

Bausch, W.C. 1995. Remote sensing of crop coefficients for improving the irrigation scheduling of corn. *Agricultural Water Management* 27:55–68.

Brutsaert, W., and D. Chen. 1996. Diurnal variation of surface fluxes during thorough drying (or severe drought) of natural prairie. *Water Resource Research* 32:2013–19.

CALMIT. 2006. Delineation of 2005 land use patterns for the state of Nebraska Department of Natural Resources in the central Platte river basin. Final Report, Center for Advanced Land Management Information Technologies (CALMIT), University of Nebraska–Lincoln.

Church, M.R., G.D. Bishop, and D.L. Cassell. 1995. Maps of regional evapotranspiration and runoff/precipitation ratios in the northeast United States. *Journal of Hydrology* 168:283–98.

Crawford, T.M., and C.E. Duchon. 1999. An improved parameterization for estimating effective atmospheric emissivity for use in calculating daytime downwelling longwave radiation. *Journal of Applied Meteorology* 38:474–80.

Diak, G.R., W.L. Bland, J.R. Mecikalski, and M.C. Anderson. 2000. Satellite-based estimates of long-wave and solar radiation for agricultural applications. *Agricultural and Forest Meteorology* 103:349–55.

Franks, S.W., and K.J. Beven. 1997a. Bayesian estimation of uncertainty in land surface atmosphere flux predictions. *Journal of Geophysical Research* 102:991–99.

Franks, S.W., and K.J. Beven. 1997b. Estimation of evapotranspiration at the landscape scale: A fuzzy disaggregation approach. *Water Resources Research* 33:2929–38.

Franks, S.W., and K.J. Beven. 1999. Conditioning a multiple-patch SVAT model using uncertain time–space estimates of latent heat flux as inferred from remotely sensed data. *Water Resources Research* 35:2751–61.

Goodrich, D.C., R. Scott, J. Qi, B. Goff, C.L. Unkrich, M.S. Moran, D. Williams, S. Schaeffer, K. Snyder, R. MacNish, T. Maddock, D. Pool, A. Chehbouni, D.I. Cooper, W.E. Eichinger, W.J. Shuttleworth, Y. Kerr, R. Marsett, and W. Ni. 2000. Seasonal estimates of riparian evapotranspiration using remote and in situ measurements. *Agricultural and Forest Meteorology* 105:281–309.

Irmak, A., and S. Irmak. 2008. Reference and crop evapotranspiration in south central Nebraska: II. Measurement and estimation of actual evapotranspiration for corn. 2008. Measurement and estimation of actual evapotranspiration. *Journal of Irrigation and Drainage Engineering* 134:700–715.

Irmak, A., S. Irmak, and D.L. Martin. 2008. Reference and crop evapotranspiration in south central Nebraska: I. Comparison and analysis of grass and alfalfa-reference evapotranspiration. *Journal of Irrigation and Drainage Engineering* 134:690–99.

Irmak, A., and B. Kamble. 2009. Evapotranspiration data assimilation with genetic algorithms and SWAP model for on-demand irrigation. *Irrigation Science.* 28:101–12.

Jacobs, J.M., M.C. Anderson, L.C. Friess, and G.R. Diak. 2004. Solar radiation, longwave radiation, and emergent wetland evapotranspiration estimates from satellite data in Florida, USA. *Hydrological Sciences Journal* 49:461–76.

Peacock, C.E., and T.M. Hess. 2004. Estimating evapotranspiration from a reed bed using the Bowen ratio energy balance method. *Hydrological Processes* 18:247–60.

Shuttleworth, W.J., R.J. Gurney, A.Y. Hsu, and J.P. Ormbsy. 1989. *FIFE: The Variation in Energy Partitioning at Surface Flux Sites, Remote Sensing and Large Scale Global Processes.* Proceedings of the Baltimore Symposium IAHS publication no. 186. IAHS Press, Oxfordshire, UK.

Singh, R.K., and A. Irmak. 2009. Estimation of crop coefficients using satellite remote sensing. *Journal of Irrigation and Drainage Engineering* 135:597–608.

Singh, R.K., A. Irmak, S. Irmak, and D.L. Martin. 2008. Application of SEBAL for mapping evapotranspiration and estimating surface energy fluxes in south-central Nebraska. *Journal of Irrigation and Drainage Engineering* 134:273–85.

Tasumi, M., R.G. Allen, R. Trezza, and J.L. Wright. 2003. Soil heat flux estimation method. Appendix 12 in M. Tasumi, Progress in operational estimation of regional evapotranspiration using satellite imagery. PhD diss., University of Idaho, Moscow, ID.

Tasumi, M., R.G. Allen, R. Trezza, and J.L. Wright. 2005a. Satellite-based energy balance to assess within-population variance of crop coefficient curves. *Journal of Irrigation and Drainage Engineering* 131:94–109.

Tasumi, M., R. Trezza, R.G. Allen, and J.L. Wright. 2005b. Operational aspects of satellite-based energy balance models for irrigated crops in the semi-arid US. *Irrigation and Drainage Systems* 19:355–76.

Tateishi, R., and C.H. Ahn. 1996. Mapping evapotranspiration and water balance for global land surfaces. *ISPRS Journal of Photogrammetry and Remote Sensing* 51:209–15.

Trezza, R., R.G. Allen, M. Tasumi, and J.L. Wright. 2003. Observed ETrF and EF values. Appendix 13 in M. Tasumi, Progress in operational estimation of regional evapotranspiration using satellite imagery. PhD diss., University of Idaho, Moscow, ID.

Verma, S.B., J. Kim, and R.J. Clement. 1992. Momentum, water vapor, and carbon dioxide exchange at a centrally located Prairie site during FIFE. *Journal of Geophysical Research* 97(D17):18629–39.

Wang, J., Y. Ma, M. Menenti, W.G.M. Bastiaanssen, and Y. Mitsuta. 1995. The scaling up of processes in the heterogeneous landscape of HEIFE in full with the aid of satellite remote sensing. *Journal of the Meteorological Society of Japan* 73:1235–44.